Computation of Rotating Turbulent Flow with an Algebraic Reynolds Stress Model

Matthew J. Warfield* and B. Lakshminarayana†
The Pennsylvania State University, University Park, Pennsylvania

Rotation has a strong effect on the structure of turbulent flows. Turbulence models based on isotropic eddy viscosity are ineffective at predicting such flows. An algebraic Reynolds stress model has been implemented to modify the Kolmogorov-Prandtl eddy-viscosity relation to produce an anisotropic turbulence model. The eddy-viscosity relation becomes a function of the local turbulent production-dissipation ratio and local turbulence/rotation parameters. A three-dimensional model is presented, and a two-dimensional form is utilized to predict fully developed rotating channel flow over a wide range of rotation numbers. In addition, predictions are obtained for a developing channel flow with high rotation. The predictions are compared with available experimental data. Good predictions are achieved for mean velocity and wall shear stress over most of the rotation speeds tested. There is some prediction breakdown at high rotation (Ω greater than 0.10), where the effects of the rotation on turbulence become quite complex. At high rotation and low Reynolds number, laminarization on the trailing side of the channel represents a complex effect of rotation that is difficult to predict with the described models.

Nomenclature

A, C = constants in law of wall relation
C_μ = eddy-viscosity coefficient
d = channel width
g_{ijkm} = mean velocity derivative ratios defined in Eq. (18)
k = turbulence kinetic energy $= (\overline{u_i u_i})/2$
p = static pressure normalized by ρU^2
P = production of kinetic energy, defined in Eq. (4)
q = unknown vector $= [p, U, V]$
Re = Reynolds number $= U_m d/\nu$
r_k, r_{ijk} = turbulence parameters defined in Eq. (18)
U_i, U, V = mean velocities normalized by U_m
U_* = wall shear velocity $= (\tau_0)^{1/2}$
U^+ = wall velocity variable $= U/U_*$
u_i, u, v = velocity fluctuations
$\overline{u_i u_j}$ = Reynolds stress tensor normalized by U_m^2
x_i = coordinate directions
y = distance normal to leading side (Fig. 1) normalized by d
y^+ = wall length variable $= yU_* Re$
δ_{ij} = Kronecker delta
ϵ = dissipation of turbulence kinetic energy
ϵ_{ijk} = alternating tensor
κ = von Kármán constant
ν = kinematic viscosity
ν_t = eddy viscosity
ρ = density
σ = small negative coefficient for space marching
τ_0 = normalized wall shear stress $= [\partial U/\partial y]_0 Re$
ω = rotation rate, 1/s
Ω = rotation number $= \omega d/U_m$

Subscripts

δ = values at edge of boundary layer
ϵ = dissipation equation
k = kinetic energy equation
m = average
p = modification of pressure for space marching
s = slip
σ = modification of vector for space marching
0 = wall value
1 = first grid point from wall

Introduction

MANY practical turbulent flows (see Fig. 1 for examples) are three-dimensional, rotating, and subject to curvature. The present state of turbulence modeling for complex flows[1] prohibits the simultaneous examination of these features, but relevant advances through studies of the individual phenomena could eventually lead to effective models incorporating all these features. The subject of this paper is the analysis and prediction of turbulent flows where rotation is the dominant feature. This is achieved through the use of an algebraic Reynolds stress model for the turbulence.

There is considerable experimental evidence attesting to the degree to which rotation affects turbulence.[2-5] Principal among these effects are the stabilizing/destabilizing characteristics of rotating boundary layers due to imposed Coriolis accelerations. Also important are variations in the production to dissipation ratio, with a corresponding effect on turbulence and mean flow quantities.

Prediction of rotating turbulent flows requires an extension of simple isotropic eddy viscosity:

$$-\overline{u_i u_j} = \nu_t \left(\frac{\partial U_i}{\partial x_j} + \frac{\partial U_j}{\partial x_i} \right) - \left(\frac{2}{3} \right) \delta_{ij} k \qquad (1)$$

The assumption of isotropic eddy viscosity implies that the Reynolds stress tensor is aligned with the mean strain rate tensor, with eddy viscosity as a constant of proportionality. Predictions of turbulent rotating flows with simple eddy-viscosity models have accounted for rotation through mixing length models,[6] modified two-equation models,[7,8] and

Presented as Paper 86-0214 at the AIAA 24th Aerospace Sciences Meeting, Reno, NV, Jan. 6-9, 1986; received Feb. 12, 1986; revision received June 6, 1986.

*NASA CFD Trainee, Department of Aerospace Engineering. Student Member AIAA.

†Evan Pugh and Distinguished Alumni Professor of Aerospace Engineering; also Director, Computational Fluid Dynamics Studies, Department of Aerospace Engineering. Fellow AIAA.

algebraic stress models.[9-11] The algebraic stress models, in general, allow the incorporation of more flow physics because the ad hoc nature of the development is minimized.

The algebraic Reynolds stress model (ARSM) was originally proposed in general form by Rodi.[12] Galmes and Lakshminarayana[13] developed an ARSM that incorporated rotational effects. Full Reynolds stress models (RSM) show promise for rotational flows but are expensive to solve in practical situations.

This paper presents a variable C_μ model for the turbulence based on the ARSM of Ref. 13 and shows its application in a two-dimensional Navier-Stokes code. The model is applied to two sets of two-dimensional rotating channel flow data: one fully developed flow and the other developing flow, at a variety of Reynolds numbers. In addition, the importance of certain processes in rotating turbulent flow will be emphasized and an evaluation of the proposed model put forth.

Mean Flow Governing Equations

The governing equations for the Reynolds-averaged Navier-Stokes equations can be written as

$$\frac{S\partial q}{\partial t}+\frac{\partial E}{\partial x}+\frac{\partial F}{\partial y}+\frac{\partial G}{\partial z}-\left(\frac{1}{Re}\nabla^2 Sq\right)=[0,B] \qquad (2)$$

where

$$q=[p,U,V,W], \quad E=[U,U^2+p,UV,UW]$$

$$F=[V,UV,V^2+p,VW], \quad G=[W,UW,VW,W^2+p]$$

$$S=\text{diag}(0,1,1,1)$$

$$B=[-2\epsilon_{ijk}\Omega_j U_k-(\Omega_m x_m\Omega_i-\Omega_n\Omega_n x_i)-\partial\overline{u_iu_j}/\partial x_j]$$

(Here, the first equation is continuity while the last three represent the x, y, and z momentum equations.) The Reynolds stress in term B of Eq. (2) may be evaluated directly using ARSM or RSM models or by utilizing an eddy viscosity from Eq. (1).

Turbulence Modeling

Two-Equation Model

A standard two-equation model is utilized to solve for turbulence velocity and length scales utilizing an equation for kinetic energy and dissipation as follows:

k-ϵ model:

$$\frac{\partial A_T}{\partial x}+\frac{\partial B_T}{\partial y}+\frac{\partial C_T}{\partial z}=\frac{1}{Re}\left(\frac{\partial C_{T1}}{\partial x}+\frac{\partial C_{T2}}{\partial y}+\frac{\partial C_{T3}}{\partial z}+D_T\right) \qquad (3)$$

where

$$A_T=[Uk,U\epsilon], \quad B_T=[Vk,V\epsilon], \quad C_T=[Wk,W\epsilon]$$

$$C_{T1}=\left[\nu_k\frac{\partial k}{\partial x},\ \nu_\epsilon\frac{\partial\epsilon}{\partial x}\right], \quad C_{T2}=\left[\nu_k\frac{\partial k}{\partial y},\ \nu_\epsilon\frac{\partial\epsilon}{\partial y}\right]$$

$$C_{T3}=\left[\nu_k\frac{\partial k}{\partial z},\ \nu_\epsilon\frac{\partial\epsilon}{\partial z}\right]$$

$$D_T=[P-\epsilon, C_{\epsilon1}P\epsilon/k-C_{\epsilon2}\epsilon^2/k]$$

$$\nu_k=1+(\nu_t/\sigma_k), \quad \nu_\epsilon=1+(\nu_t/\sigma_\epsilon)$$

$$C_{\epsilon1}=1.44, \quad C_{\epsilon2}=1.92, \quad \sigma_k=1.0, \quad \sigma_\epsilon=1.3$$

To avoid the necessity for near-wall modeling, k and ϵ at the first grid point could be obtained using local equilibrium assumptions if the first grid point is placed in the inertial sublayer. These establish k and ϵ at the first grid point using the following relations:

$$k_1=\left(\frac{U_*^2}{\sqrt{C_\mu}}\right) \qquad \epsilon_1=\frac{U_*^3}{\kappa y_1}$$

Algebraic Reynolds Stress Model

A full Reynolds stress model includes transport partial differential equations for the Reynolds stresses, which require a considerable computational effort to solve. The terms that make the Reynolds stress transport equations differential equations are the convection and diffusion terms. Rodi[12] proposed linking these terms to other known quantities by assuming that the transport of the Reynolds stresses is proportional to the transport of kinetic energy. This reduces the equations to an algebraic form with a commensurate increase in the ease of solution. The ARSM of Rodi is

$$\frac{\overline{u_iu_j}}{k}=\frac{2}{3}\delta_{ij}+\frac{(P_{ij}-2P\delta_{ij}/3)(1-C_2)}{P+\epsilon(C_1-1)} \qquad (4)$$

where

$$P_{ij}=(-\overline{u_iu_k}U_{j,k}-\overline{u_ju_k}U_{i,k}), \quad 2P=P_{ii},$$

$$C_1=1.5, \quad C_2=0.6$$

The ARSM for rotating turbulent flows[13] was derived by making the same assumptions that Rodi made but for the Reynolds stress equations with rotational terms. The model is

$$\frac{\overline{u_iu_k}}{k}=\frac{2}{3}\delta_{ik}+\frac{R_{ik}(2-C_2)/2+(P_{ik}-2P\delta_{ik}/3)(1-C_2)}{P+\epsilon(C_1-1)} \qquad (5)$$

where

$$R_{ik}=-2\Omega_p(\epsilon_{ipj}\overline{u_ku_j}+\epsilon_{kpj}\overline{u_iu_j})$$

For important rotating flows (Fig. 1) at a high Reynolds number in the x_1 direction, the important velocity derivatives are $\partial U/\partial y$ for the channel, $\partial U/\partial y$ and $\partial U/\partial z$ for the duct, and $\partial U/\partial y$, $\partial U/\partial z$, $\partial W/\partial y$, and $\partial V/\partial z$ for axial turbomachinery. When Eq. (5) is simplified, mean velocity derivatives other than the four listed above are dropped; arbitrary rotation is maintained to yield the following stress equations in which mean flow quantities are written in terms of (U,V,W), while the Reynolds stresses are written using

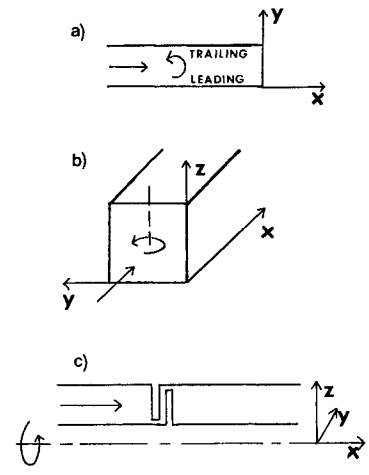

Fig. 1 Rotating flow geometries: a) channel; b) duct; c) axial turbomachinery.

Cartesian tensor notation following Eq. (5), with (1,2,3) corresponding to the (x,y,z) directions:

$$\frac{\overline{u_1u_1}}{k}=\frac{2}{3}+\frac{2(\Omega_3\overline{u_1u_2}-\Omega_2\overline{u_1u_3})(2-C_2)}{P+\epsilon(C_1-1)}+\frac{(C_2-1)[(2\overline{u_1u_2}\partial U/\partial y+2\overline{u_1u_3}\partial U/\partial z)+2P/3]}{P+\epsilon(C_1-1)} \tag{6}$$

$$\frac{\overline{u_2u_2}}{k}=\frac{2}{3}+\frac{2(\Omega_3\overline{u_1u_2}-\Omega_1\overline{u_2u_3})(2-C_2)+2(C_2-1)(P/3+\overline{u_2u_3}\partial V/\partial z)}{P+\epsilon(C_1-1)} \tag{7}$$

$$\frac{\overline{u_3u_3}}{k}=\frac{2}{3}+\frac{2(\Omega_2\overline{u_1u_3}-\Omega_1\overline{u_2u_3})(2-C_2)+2(C_2-1)(P/3+\overline{u_2u_3}\partial W/\partial y)}{P+\epsilon(C_1-1)} \tag{8}$$

$$\frac{\overline{u_1u_2}}{k}=\frac{[\Omega_3(\overline{u_2u_2}-\overline{u_1u_1})+\Omega_1\overline{u_1u_3}-\Omega_2\overline{u_2u_3}](2-C_2)}{P+\epsilon(C_1-1)}+\frac{(C_2-1)(\overline{u_2u_2}\partial U/\partial y+\overline{u_2u_3}\partial U/\partial z+\overline{u_1u_3}\partial V/\partial z)}{P+\epsilon(C_1-1)} \tag{9}$$

$$\frac{\overline{u_1u_3}}{k}=\frac{[\Omega_2(\overline{u_1u_1}-\overline{u_3u_3})+\Omega_3\overline{u_2u_3}-\Omega_1\overline{u_1u_2}](2-C_2)}{P+\epsilon(C_1-1)}+\frac{(C_2-1)(\overline{u_3u_3}\partial U/\partial z+\overline{u_2u_3}\partial U/\partial y+\overline{u_1u_2}\partial W/\partial y)}{P+\epsilon(C_1-1)} \tag{10}$$

$$\frac{\overline{u_2u_3}}{k}=\frac{[\Omega_1(\overline{u_3u_3}-\overline{u_2u_2})+\Omega_2[\overline{u_1u_2}-\Omega_3\overline{u_1u_3}](2-C_2)}{P+\epsilon(C_1-1)}+\frac{(C_2-1)(\overline{u_2u_2}\partial W/\partial y+\overline{u_3u_3}\partial V/\partial z)}{P+\epsilon(C_1-1)} \tag{11}$$

In Eqs. (6–11),

$$P=-[\overline{u_1u_2}\partial U/\partial y+\overline{u_1u_3}\partial U/\partial z+\overline{u_2u_3}(\partial V/\partial z+\partial W/\partial y)]$$

Note the effects of rotation on the Reynolds stresses. Turbulence energy is transferred from streamwise intensities to normal intensities, as evidenced by Eqs. (6) and (7) for a negative Reynolds shear stress and a positive Ω_3. Also, note that the effect on the Reynolds shear stresses depends on the relative magnitude of normal stresses. The algebraic equations are nonlinear in the Reynolds stresses and require k and ϵ, computed from their own respective transport equations. If, in a numerical simulation, the production is assumed known from a previous time or space step, the algebraic equations are reduced to linear form, the form utilized here. In principle, the results from the ARSM in the form of the Reynolds shear stresses would be utilized to close the Reynolds-averaged momentum equations to allow a solution for the mean flow. Unfortunately, many mean flow solution procedures often experience numerical instability with this source term type of closure. In addition, the assumptions made in reducing the Reynolds stress equations from differential to algebraic form compromise the quantitative accuracy of the turbulent stress prediction. There are methods available to enhance the numerical stability of the closure scheme. One of these is the variable C_μ modification to the k-ϵ model.

C_μ Modified for Rotation and Three-Dimensionality

A successful ARSM implementation approach[10,14,15] is the modification of the transport coefficient C_μ in the Kolmogorov-Prandtl relation to account for the results of the ARSM. This effectively becomes a modification of the k-ϵ model which, while not representing physical processes perhaps as well as a Reynolds stress model, is well tested and inherently stable over a wide range of flows.

By introducing the assumption of local equilibrium ($P=\epsilon$) and two-dimensionality in Eqs. (6), (7), and (9) for a rotating channel, Pouagare and Lakshminarayana[10] developed the relation

$$C_\mu=0.9+\Omega\Big/\frac{\partial U}{\partial y} \tag{12}$$

This relation is similar to the Richardson number approach[3]: $Ri=S(S+1)$

where

$$S=-2\Omega\Big/\frac{\partial U}{\partial y} \tag{13}$$

These relations (where Ω is Ω_3) give the desired enhancement of turbulence on the leading side and suppression at the trailing side but also result in a discontinuity at the centerline of the channel, where the velocity gradient changes sign.

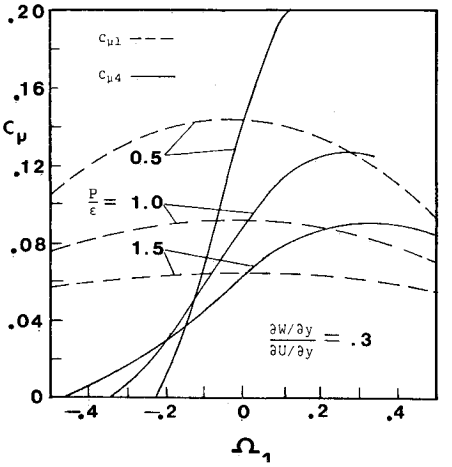

Fig. 2 Distribution of C_μ with rotation for hypothetical axial turbomachinery flow.

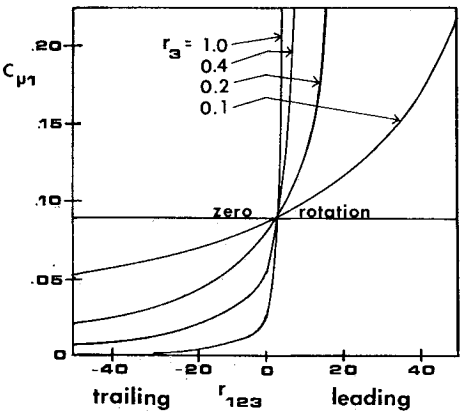

Fig. 3 Distribution of $C_{\mu 1}$ with rotation parameters for a rotating channel with production equal to dissipation.

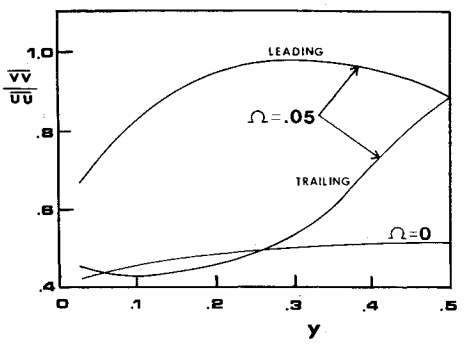

Fig. 4 Variation of the ratio of normal to streamwise turbulence intensity in a rotating channel; $Re = 57{,}000$.

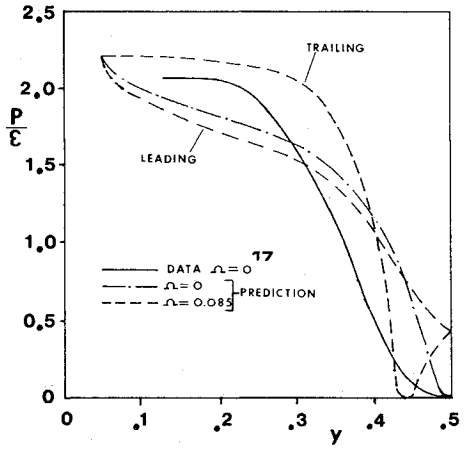

Fig. 5 Effects of rotation on production-dissipation ratio for a rotating channel; $Re = 57{,}000$.

In this paper, the analysis has been extended to the general three-dimensional, nonequilibrium case. By neglecting nonlinear combinations of rotation numbers except for Ω_1^2 and Ω_3^2 (Ω_3 is the principal rotation for rotating duct flows, while Ω_1 is the principal rotation for turbomachinery flows), Eqs. (6–11) can be solved in closed form to yield relations for the Reynolds shear stresses.

The full C_μ relations (where C_μ now is a vector) are presented in Eqs. (14–17). The terms are given in the Appendix.

$$C_{\mu 1} = A_1 d + A_2 d g_{1312} + A_3 d(g_{2312} + g_{3212}) \tag{14}$$

$$C_{\mu 2} = B_1 d g_{1213} + B_2 d + B_3 d(g_{2313} + g_{3213}) \tag{15}$$

$$C_{\mu 3} = F_1 d g_{1223} + F_2 d g_{1323} + F_3 d(1 + g_{3223}) \tag{16}$$

$$C_{\mu 4} = F_1 d g_{1232} + F_2 d g_{1332} + F_3 d(1 + g_{2332}) \tag{17}$$

The C_μ vector is applied as follows to close the Reynolds-averaged equations:

$$-\overline{u_1 u_2} = C_{\mu 1} \frac{k^2 \partial U}{\epsilon \partial y}, \quad -\overline{u_1 u_3} = C_{\mu 2} \frac{k^2 \partial U}{\epsilon \partial z},$$

$$-\overline{u_2 u_3} = C_{\mu 3} \frac{k^2 \partial V}{\epsilon \partial z} + C_{\mu 4} \frac{k^2 \partial W}{\epsilon \partial y}$$

The split treatment of $C_{\mu 3}$ and $C_{\mu 4}$, while not following the eddy-viscosity principle, is necessary for implementation of the variable C_μ model into the momentum equations, where the following terms require closure:

x momentum:

$$-\left(\frac{\partial \overline{u_1 u_2}}{\partial y} + \frac{\partial \overline{u_1 u_3}}{\partial z}\right)$$

y momentum:

$$-\frac{\partial \overline{u_2 u_3}}{\partial z}$$

z momentum:

$$-\frac{\partial \overline{u_2 u_3}}{\partial y}$$

The following natural groups appear in Eqs. (14–17):

$$\frac{P}{\epsilon}, \quad r_k = \frac{k\Omega_k}{\epsilon}, \quad r_{ijk} = \frac{\partial U_i}{\partial x_j} \Big/ \Omega_k, \quad g_{ijkm} = \frac{\partial U_i}{\partial x_j} \Big/ \frac{\partial U_k}{\partial x_m} \tag{18}$$

The three-dimensional variable C_μ model was utilized with a test case in which $\partial U/\partial y$ and $\partial W/\partial y$ (with $C_{\mu 1}$ and $C_{\mu 4}$) terms were retained while other mean velocity derivatives were dropped. Figure 2 shows the distribution of $C_{\mu 1}$ and $C_{\mu 4}$ for variation in rotation number at different values of production-dissipation ratio. The effect on $C_{\mu 1}$ is slight, especially at higher P/ϵ values, while a general increase is shown for $C_{\mu 4}$ in going from negative to positive rotation. These results can be explained by inclusion of the Coriolis effects in the $C_{\mu 4}$ term, which is applied to the z-momentum equation, while the streamwise flow is not directly affected by the Coriolis acceleration for this case since the rotation vector is parallel to the mean flow.

Application to Rotating Channel Flow

It is instructive to examine the case of two-dimensional rotating channel flow (Fig. 1), where the result reduces to

$$C_{\mu 1} = -\frac{(2/3)(C_2 - 1)(C_2 P/\epsilon + C_1 - 1)}{D_1 + D_2} \tag{19}$$

where

$$D_1 = (P/\epsilon)^2 + 2(P/\epsilon)(C_1 - 1) + (C_1 - 1)^2$$

$$D_2 = [4r_3(2 - C_2)/2]^2 + 4(C_2 - 1)(2 - C_2) r_3^2 r_{123}$$

Equation (19) effectively gives $C_{\mu 1}$ as a function of P/ϵ, r_3, and r_{123}. Using values for the constants of $C_1 = 1.5$ and $C_2 = 0.6$, Eq. (19) yields $C_{\mu 1}$ to be approximately 0.13 for the nonrotating local equilibrium case. It was determined to force the coefficient to be the standard value of 0.09 for the zero rotation, local equilibrium case. The altered form of the relation is then obtained by multiplying Eq. (19) by the factor 0.09/0.13. The importance of the production–dissipation ratio is readily visible in this reduced equation. Note the effect of rotation on $C_{\mu 1}$. For $r_{123} > 0$ (leading side), $C_{\mu 1}$ is enhanced, while for $r_{123} < 0$ (trailing side), $C_{\mu 1}$ is decreased. Additionally, this formulation provides a continuous distribution of $C_{\mu 1}$ across the flowfield, a physically realistic result. Figure 3 shows the distribution of $C_{\mu 1}$ with the turbulence rotation parameters for a local equilibrium situation. In general, r_3 is largest away from the walls, while r_{123} is largest near the walls. The leading-side effect is much more dominant. This appears to be supported by the eddy-viscosity profiles of Johnston et al.,[3] where the unstable side was shown to have a stronger variation in eddy viscosity. The realizability of $C_{\mu 1}$ is ensured by setting the following limits:

$$C_{\mu 1}(\max) = 0.200, \quad C_{\mu 1}(\min) = 0.025$$

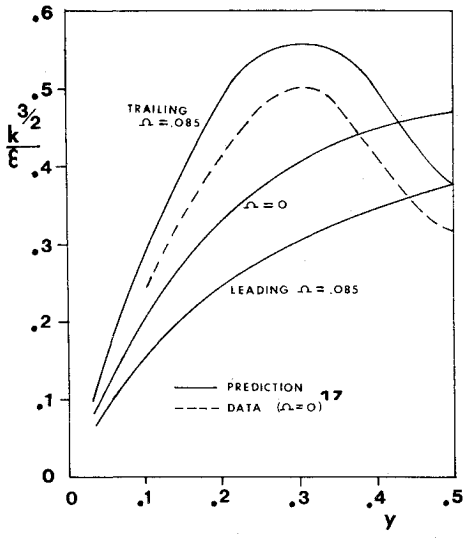

Fig. 6 Effects of rotation on turbulence length scale for a rotating channel; $Re = 57{,}000$.

The ARSM closure and modified C_μ models were implemented in a two-dimensional space-marching code for application to two-dimensional rotating channel flow, where only $C_{\mu 1}$ is active and where the source vector of the mean momentum equations reduces to:

$$B = \left[0, 2\Omega_3 V + \Omega_3^2 x - \frac{\partial \overline{u_1 u_2}}{\partial y}, \quad -2\Omega_3 U + \Omega_3^2 y\right]$$

The two-dimensional version of Eq. (2) is reduced to space-marching form by neglecting streamwise diffusion and by splitting the pressure into an assumed part and an implicit part.[16] The use of a small coefficient σ on the implicit pressure enables the system to be marched parabolically. The resulting modified vectors are

$$E_\sigma = [U, U^2 + \sigma p, UV], \quad E_p = [0, -\sigma p + p, 0]$$

The coefficient $\sigma(=-0.01)$ is introduced to change the character of the equation from elliptic to hyperbolic. The coupled solution is achieved through single-pass streamwise integration via the standard Euler-implicit solution procedure. More details on the solution procedure can be found in Ref. 16. The equations are presented in Cartesian form but are equally applicable in generalized body-fitted coordinates. Details on the turbulene model implementation to follow.

Because of better prediction performance obtained, a turbulence slip velocity was used in most instances rather than a no-slip boundary condition. Cases in which laminarization of the channel trailing side occurred were also predicted using a no-slip boundary condition on that side only. The slip velocity was set by using the law-of-the-wall form

$$U/U_* = A \log y^+ + C$$

For the applications considered, $A = 5.8$ and $C = 5$. From the friction velocity, the slip velocity was determined from

$$U_s = U_1 - (U_*/\kappa)$$

There is evidence[5] that rotation affects the law-of-the-wall distribution for fully turbulent flow, but the effects are greatest for $y^+ > 100$. The grid for the problems encountered was set so that the first grid point was in the 20–30 range of y^+, for which it was assumed the standard law of the wall was valid.

Initial conditions for mean velocity were set from the data, if available, or from mass flow conditions with a uniform inlet profile.

Numerical Results and Analysis

The two-dimensional ARSM [Eqs. (6), (7), and (9)] was applied to rotating channel flow. The ARSM was solved to yield the Reynolds stress that was included in the mean momentum equation through the source term B in Eq. (2). Later discussion will refer to this as the ARSM closure scheme. The solution procedure for the ARSM closure method was as follows:

1) Solve for k and ϵ at the previous streamwise station using the mean velocity solution at that station.

2) Use k and ϵ values to solve the algebraic stress equations at the previous station.

3) Use Reynolds shear stress to close the mean flow equations at the current station.

When the modified C_μ method was used, k and ϵ at the previous station were utilized, along with $C_{\mu 1}$, to close the mean flow equations at the current station through the eddy viscosity.

It was found that the ARSM closure method tended to be unstable for rotation numbers greater than about 0.05. Solutions could be obtained for higher rotation rates, but spatial oscillations occurred in the results. Despite the instability, several results were obtained with the ARSM closure scheme at low rotation. Figure 4 shows the ratio of normal to streamwise turbulence intensities for zero rotation and also for low rotation ($\Omega_3 = 0.05$). The increase with rotation of the normal intensities and the decrease of streamwise intensities on the leading side are reflected in the results and represent the transfer of turbulence energy, as discussed earlier. The results shown in Fig. 4 are consistent with the data of Koyama et al.[5] (see their Fig. 13) in that the ratio of the normal component of turbulence intensity to the streamwise component is greater with rotation than without rotation over most of the flowfield.

Comparisons were made for streamwise velocity and Reynolds stress profiles for zero rotation cases measured by Laufer[17] and Halleen and Johnston,[18] with good results shown.[19] Figure 5 shows the effect of rotation on the production-dissipation rate. Although quantitative features of this ratio are difficult to predict (and measure), the overall effect of rotation appears principally on the trailing side with an enhanced production-dissipation ratio. Leading-side effects, while opposite from trailing-side effects, are not as marked. The shift of the zero slope point in the velocity profile from the center of the channel to the trailing side creates altered effects near $y = 0.5$. Figure 6 shows the length-scale parameter $k^{3/2}/\epsilon$ and its distribution with and without rotation. The zero rotation prediction does not match the data well because of the slower rate of decrease in the dissipation as the center of the channel is approached. The effects of rotation are seen in the decreased length scale on the leading side and increased length scale on the trailing side. Both the energy balance and the length-scale results of Figs. 5 and 6 are mostly effected by changes in the dissipation rate with rotation. Since production of kinetic energy is enhanced near the leading side, and since the production-dissipation ratio and turbulence length scale are lower near the leading side than near the trailing side, it can be inferred that rotation has a greater effect on dissipation than it does on kinetic energy or production of kinetic energy. Figures 4–6 concern diagnostic results obtained with the ARSM closure scheme, where later results concern the modified C_μ closure scheme for the two-dimensional rotating channel.

Fully developed two-dimensional flow in a rotating channel was measured by Halleen and Johnston.[18] The experiment included a variety of Reynolds number/rotation number combinations. Their rotating duct of high aspect ratio was 59 in. long and 1.5 in. wide. Water flow was used

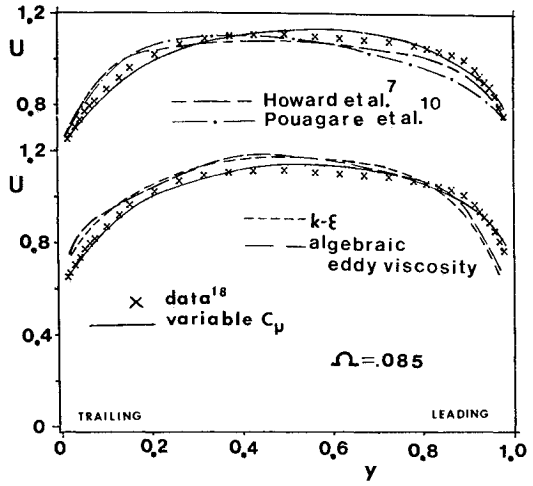

Fig. 7 Comparison of velocity profiles resulting from modified and unmodified turbulence models for a flow in a rotating channel; $Re = 35{,}000$.

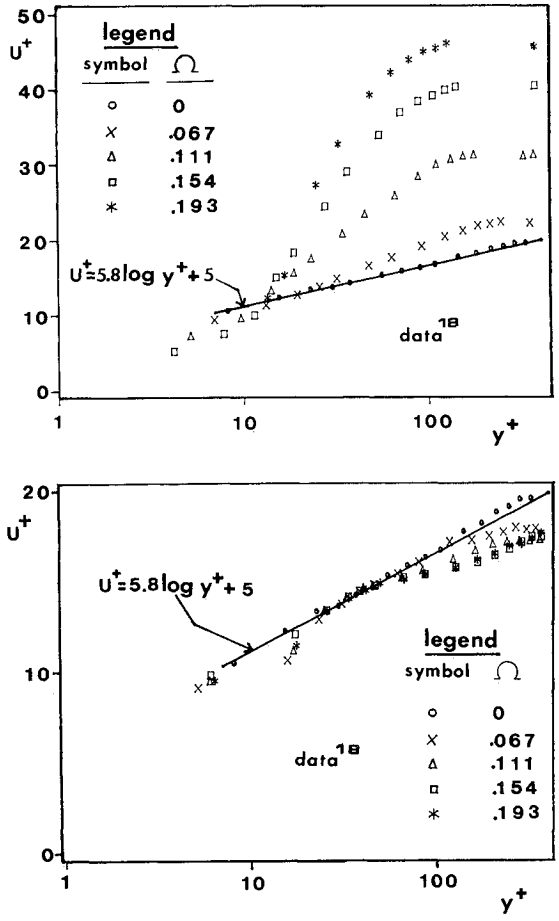

Fig. 8 Law-of-the-wall velocity plots for flow in a rotating channel; $Re = 11{,}500$: a) trailing side; b) leading side.

in the channel and Reynolds numbers in the 11,000–35,000 range were used in conjunction with rotation numbers in the 0–0.2 range. The measurements were taken 29–34 channel widths downstream of the inlet (depending on the case). The stable variable C_μ turbulence model was applied to several of the cases, whereas the ARSM closure scheme was utilized only at zero rotation because of its stability limitations. The solution was started from the channel inlet and utilized uniform inlet conditions. Figure 7 shows high Reynolds

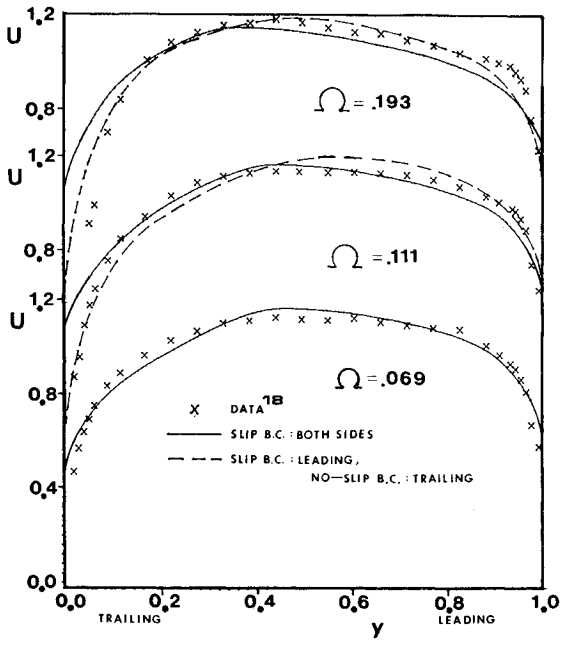

Fig. 9 Comparison of rotating channel velocity profiles with data using different boundary conditions; $Re = 11{,}500$.

number predictions of mean velocity for a moderate rotation value, comparing the variable C_μ method with unmodified standard models and with other modified two-equation models. It can be seen that the prediction from the variable C_μ model is superior to those from unmodified standard zero and two-equation models. The variable C_μ prediction also appears favorable to the other modified two-equation models.

The lower Reynolds number data of Halleen and Johnston show a laminarization of the flow near the trailing side at higher rotation numbers. Figure 8, where Halleen and Johnston's data are shown plotted in law-of-the-wall form, shows the dramatic effect on the law-of-the-wall assumption. Note that fully turbulent flow still exists on the leading side, while laminar flow arises on the trailing side for higher rotation numbers. Since the flow is laminarizing near the trailing side, assumptions related to high Reynolds number conditions are no longer valid. This invalidates both the wall function boundary-condition approach and the high Reynolds number two-equation model in use. Predictions were attempted with the discussed model, however, as a first step, by using both wall functions (assuming the log-law to hold and remain unaltered with rotation) and by utilizing no-slip boundary conditions for the trailing side while continuing to use the slip velocity on the leading side. In both cases, wall functions were utilized for k and ϵ at the walls. Figure 9 shows a series of predictions at lower Reynolds number over a wide range of Ω, comparing the two approaches. Much better agreement is shown when the no-slip boundary condition is used on the trailing side, but it must be emphasized that this type of situation demands the application of near-wall/low Reynolds number modeling. The no-slip treatment on the trailing side appears to improve the prediction at higher rotation, probably because of the increasing laminar zone, which makes the no-slip boundary condition a better choice with the grid placements used. The data at the highest rotation number show a large boundary-layer growth in conjunction with high wall shear stress on the leading side; this is a complex turbulence effect that is difficult to capture. The laminarization of the trailing side at low Reynolds number has been discussed in Refs. 3 and 4.

Figure 10 shows the variation of predicted wall shear velocity with rotation for the Halleen and Johnston data. The comparison with modified and unmodified models is again

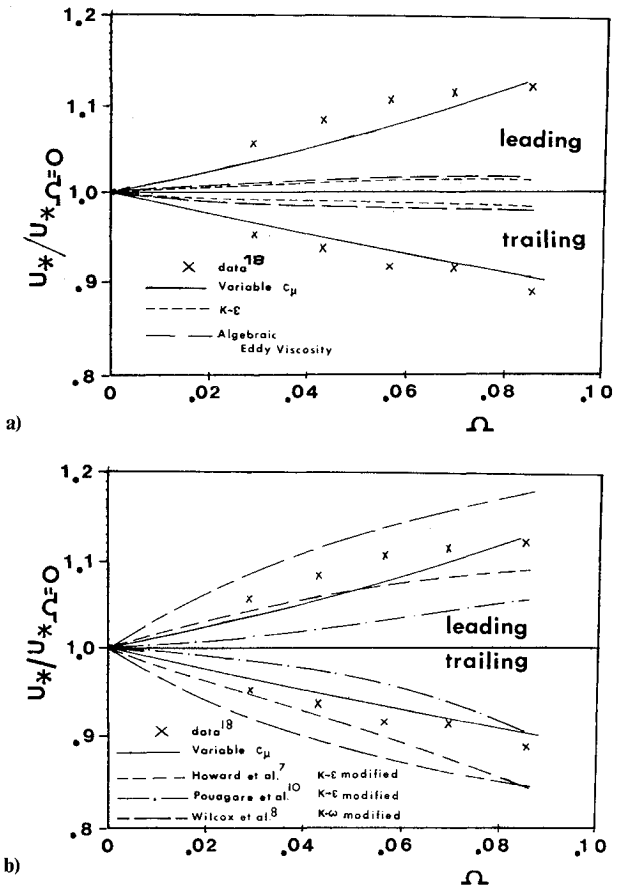

Fig. 10 Wall shear velocity variation in a rotating channel; $Re = 35{,}000$: a) comparison between modified and unmodified models; b) comparison between modified models.

favorable to the present method. The C_μ implementation of the ARSM has been effective at predicting the correct rotation effect on wall shear stress.

The Halleen-Johnston channel cases were predicted with 40 cross-channel points. The solution with the standard k-ϵ model for 105 streamwise stations required approximately 22-s CPU time on an IBM 3081. The variable C_μ model took negligibly greater time, while the pure ARSM required an additional 2-s CPU total for the solution of the algebraic stress equations at each grid point. The space-marching algorithm, coupled with the k-ϵ/variable C_μ turbulence model, represents a very economical solution procedure. The variable C_μ model proved to be sensitive to the ratio of production to dissipation in some regions, and smoothing of this ratio across the channel was utilized to stabilize the solution procedure.

Koyama et al.[4] have measured a developing turbulent channel flow at high rotation. Their channel utilized airflow through a high-aspect-ratio duct with a length of 280 mm and a width of 40 mm. Rotation numbers ranging from 0 to 0.25 were used. The modified C_μ model was applied to that case and predictions were for $\Omega_3 = 0.25$. Figure 11 shows mean velocity predictions at several stages of development of the rotating flow. Although the profile is reasonably well predicted, the growth of the boundary layer is not well predicted. In addition, the sharp corner in the profile near the leading side at the final predicted station has not been captured. At this high rotation value, it is seen that the prediction becomes somewhat poorer as the development continues. There is the same laminarization effect in this case that was seen in the previous low Reynolds number case. The laminarization here occurs at higher Reynolds number and at a higher rotation number than in the previous case and becomes more pronounced with streamwise distance. The

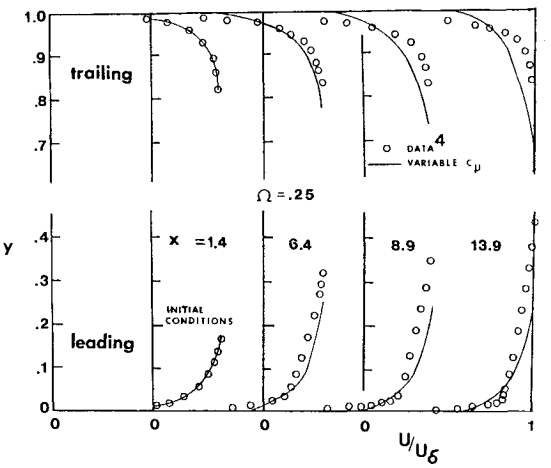

Fig. 11 Velocity predictions for a developing rotating channel flow; $Re = 16{,}500$.

same turbulence mechanisms near the leading side appear to be in operation for this case as in the previous cases: high wall shear stress, coupled with increasing boundary-layer growth, with higher rotation rates. It appears that the performance of the model deteriorates when fully developed conditions create interaction between the boundary layers on the leading and trailing sides.

Conclusions

An algebraic Reynolds stress model has been formulated for general three-dimensional rotating turbulent flows of the type found in rotating ducts and turbomachinery. A modified C_μ method of implementation gave good velocity and wall shear stress predictions over a wide range of rotation numbers in a rotating channel, while an ARSM closure method gave unreliable results for all but low values of rotation. The modification of the k-ϵ model through a variable C_μ has several advantages in complex turbulence modeling:

1) It is inherently stable over a wide range of flowfields.
2) It is easy to apply to existing k-ϵ models.
3) It is computationally very efficient.
4) It is capable of extensive modification of standard k-ϵ model results.
5) When based on full Reynolds stress closures that have been reduced to algebraic form, the physical nature of rotation effects on turbulence are naturally included in contrast to ad hoc modifications.
6) Modifications based on different extra-strain effects (rotation, curvature, etc.) can be easily combined.

The variable C_μ method of application gave good velocity and wall shear stress predictions for high Reynolds number, fully developed rotating channel flows at low to moderate rotation. At lower Reynolds numbers, the tendency for the trailing side to laminarize created a prediction problem resulting from the breakdown of modeling assumptions. A developing channel flow with high rotation was well predicted in early development stages, but not as well when fully developed conditions were approached. The high wall shear stress coupled with increased boundary-layer growth on the leading side is a complex effect not well predicted by any of the models considered.

Appendix

The terms used in Eqs. (14–17) are

$$F_1 = \frac{a_1 a_2 b_2 - a_1 a_2 b_3}{G}, \quad F_2 = \frac{a_1^2 b_3 - a_1 a_2 b_1}{G},$$

$$F_3 = \frac{a_1 a_2 b_1 - a_1^2 b_2}{G}$$

$$B_1=\frac{(c_1a_2-c_2a_1)(a_1a_2b_2-a_1a_2b_3)}{H}+\frac{a_2}{a_1b_2-a_2b_1}$$

$$B_2=\frac{(a_2c_1-a_1c_2)(a_1^2b_3-a_1a_2b_1)}{H}-\frac{a_1}{a_1b_2-a_2b_1}$$

$$B_3=\frac{(c_1a_2-c_2a_1)(a_1^2b_2-a_1a_2b_1)}{H}$$

$$A_1=\frac{-1-b_1B_1-c_1C_1}{a_1},\quad A_2=\frac{-b_1B_2-c_1C_2}{a_1}$$

$$A_3=\frac{-b_1B_3-c_1C_3}{a_1}$$

$$G=(c_3a_1-c_1a_2)(a_1b_2-a_2b_1)-(b_3a_1-b_1a_2)(c_2a_1-c_1a_2)$$

$$H=G(a_1b_2-a_2b_1)$$

$$a_1=1+\frac{[2(2-C_2)r_3]^2+4(2-C_2)(C_2-1)r_3^2r_{123}}{D^2}$$

$$a_2=\frac{-(2-C_2)r_1}{D}+\frac{2(2-C_2)(C_2-1)r_2r_3r_{132}}{D^2}$$

$$-\frac{(C_2-1)r_2r_{232}}{D}-\frac{2(C_2-1)^2r_2r_3r_{123}r_{132}}{D^2}$$

$$a_3=\frac{(2-C_2)r_2}{D}-\frac{2(2-C_2)(C_2-1)r_1r_3(r_{231}-r_{123})}{D^2}$$

$$-\frac{(C_2-1)r_2r_{232}}{D}$$

$$b_1=\frac{-(C_2-1)r_1r_{321}+(2-C_2)r_1}{D}$$

$$-\frac{2(2-C_2)(C_2-1)r_2r_3r_{123}}{D^2}$$

$$b_2=1-\frac{4(2-C_2)(C_2-1)r_2^2r_{132}}{D^2}$$

$$b_3=\frac{-(2-C_2)r_3}{D}+\frac{2(2-C_2)(C_2-1)r_1r_2(r_{321}+r_{132})}{D^2}$$

$$-\frac{(C_2-1)r_3r_{123}}{D}-\frac{2(C_2-1)^2r_1r_2r_{132}r_{321}}{D^2}$$

$$c_1=\frac{-(2-C_2)r_2}{D}+\frac{(2-C_2)(C_2-1)r_1r_3r_{321}}{2D^2}$$

$$c_2=\frac{(2-C_2)r_3}{D}-\frac{2(C_2-1)(2-C_2)r_1r_2r_{231}}{D^2}$$

$$c_3=1+\frac{5(2-C_2)(C_2-1)r_1^2r_{231}}{2D^2}$$

$$-\frac{2(C_2-1)^2r_1r_2r_{321}r_{132}-2(C_2-1)^2r_1^2r_{231}r_{321}+[2(2-C_2)r_1]^2}{D^2}$$

$$d=\frac{2/3(C_2-1)}{D}+\frac{2/3(C_2-1)^2P/\epsilon}{D^2}$$

where $D=P/\epsilon+C_1-1$.

Acknowledgments

The first author was sponsored by NASA CFD Training Grant, NGT 39-009-802. The research was partially supported by NASA Grant NSG 3266, with P. Sockol as contract monitor. The authors wish to thank K. Kirtley for providing the space-marching code.

References

[1]Lakshminarayana, B., "Turbulence Modeling for Complex Flows," *AIAA Journal*, Vol. 24, Dec. 1986, pp. 1900–1917.

[2]Lakshminarayana, B. and Reynolds, B., "Turbulence Characteristics in the Near Wake of a Compressor Rotor Blade," *AIAA Journal*, Vol. 18, Nov. 1980, pp. 1354–1362.

[3]Johnston, J. P., Halleen, R. M., and Lezius, D. K., "Effects of Spanwise Rotation on the Structure of Two-Dimensional Fully Developed Turbulent Channel Flow," *Journal of Fluid Mechanics*, Vol. 56, Pt. 3, 1972, pp. 533–557.

[4]Koyama, H., Masuda, S., Ariga, I., and Watanabe, I., "Stabilizing and Destabilizing Effects of Coriolis Force on Two-Dimensional Laminar and Tubulent Boundary Layers," *Journal of Engineering for Power*, Vol. 101, Jan. 1979, pp. 23–31.

[5]Koyama, H. S. and Ohuchi, M., "Effects of Coriolis Force on Boundary Layer Development," *Proceedings of the 5th Symposium on Turbulent Shear Flows*, Ithaca, NY, Aug. 1985, pp. 21.19–21.24.

[6]Truman, C. R. and Jankowski, D. F., "Prediction of Turbulent Source Flow Between Stationary and Rotating Discs," *International Journal of Heat and Fluid Flow*, Vol. 6, No. 2, 1985, pp. 69–78.

[7]Howard, J.H.G., Patankar, S. V., and Bordynuik, R. M., "Flow Prediction in Rotating Ducts Using Coriolis-Modified Turbulence Models," *Journal of Fluids Engineering*, Vol. 102, Dec. 1980, pp. 456–461.

[8]Wilcox, D. C. and Chambers, T. L., "Streamline Curvature Effects on Turbulent Boundary Layers," *AIAA Journal*, Vol. 15, April 1977, pp. 574–580.

[9]Hah, C. and Lakshminarayana, B., "Numerical Analysis of Turbulent Wakes of Turbomachinery Rotor Blades," *Journal of Fluids Engineering*, Vol. 102, Dec. 1980, pp. 462–472.

[10]Pouagare, M. and Lakshminarayana, B., "Computation and Turbulence Closure Models for Shear Flows in Rotating Curved Bodies," *Proceedings of 4th Symposium on Turbulent Shear Flows*, Karslruhe, FRG, Sept. 1983; also *Journal of Propulsion and Power*, Vol. 2, July 1986, pp. 289–290.

[11]Lumley, J. L., Ettestad, D., and Morel, P., "Modeling the Effect of Buoyancy and Rotation on Turbulence," *International Symposium on Refined Flow Modeling and Turbulence Measurements*, University of Iowa, Sept. 1985.

[12]Rodi, W., "A New Algebraic Relation for Calculating the Reynolds Stresses," *Zeitschrift für Angewandte Mathematik und Mechanik*, Vol. 56, 1976, pp. 219–221.

[13]Galmes, J. M. and Lakshminarayana, B., "Turbulence Modeling for Three-Dimensional Shear Flows over Curved Rotating Bodies," *AIAA Journal*, Vol. 22, Oct. 1984, pp. 1420–1428.

[14]Pourahmadi, F. and Humphrey, J.A.C., "Prediction of Curved Channel Flow with an Extended k-ϵ Model of Turbulence," *AIAA Journal*, Vol. 21, Oct. 1983, pp. 1365–1373.

[15]Ljuboja, M. and Rodi, W., "Calculation of Turbulent Wall Jets with an Algebraic Reynolds Stress Model," *Journal of Fluids Engineering*, Vol. 102, Sept. 1980, pp. 350–356.

[16]Pouagare, M. and Lakshminarayana, B., "A Space-Marching Method for Viscous Incompressible Internal Flows," *Journal of Computational Physics*, Vol. 64, June 1986, pp. 389–415.

[17]Laufer, J., "Investigation of Turbulent Flow in a Two-Dimensional Channel," NACA TR-2123, 1950.

[18]Halleen, R. M. and Johnston, J. P., "The Influence of Rotation on Flow in a Long Rectangular Channel—An Experimental Study," Thermosciences Div., Dept. of Mechanical Engineering, Stanford University, Stanford, CA, Rept. MD-18, 1967.

[19]Warfield, M. J. and Lakshminarayana, B., "Computation of Turbulent Rotating Channel Flow with an Algebraic Reynolds Stress Model," AIAA Paper 86-0214, 1986.